WARSAW UNIVERSITY OF TECHNOLOGY Index 351733
FACULTY OF CIVIL ENGINEERING
COMMITTEE FOR CIVIL AND WATER ENGINEERING
POLISH ACADEMY OF SCIENCES ISSN 1230-2945

DOI: 10.24425/ace.2024.150979

ARCHIVES OF CIVIL ENGINEERING

Vol. LXX ISSUE 3 2024

 pp. 205 –224

Research paper

Influence of humidity fluctuations in the chamber on the calculated values of the moisture diffusion coefficient in wood

Anna Wicher[1], Jadwiga Świrska-Perkowska[2], Sławomir Pochwała[3]

Abstract: In civil engineering applications, alongside inherent resistance, the moisture content in wood is one of the most important factors affecting the durability of wood. The moisture content of wood is significantly influenced by the moisture diffusion coefficient. In this study, the impact of considering humidity fluctuations in a climatic chamber during the sorption process on the computational values of functional coefficients in various models of diffusion coefficient variability with material moisture content was analyzed. The dependence of the moisture diffusion coefficient on moisture concentration in wood was assumed in the form of constant, linear, quadratic, and exponential functions. The coefficients in the sought-after functions were found using the error function minimization method based on the kinetics of moisture sorption measurements in samples of Scots pine in the radial and tangential directions at an average air humidity in the chamber of 32%. As a result of the calculations, it was found that taking into account humidity fluctuations in the climatic chamber improved the fitting of computational curves to experimental curves in the case of constant and exponential models. The values of the diffusion coefficient assumed as constant calculated assuming variable humidity conditions in the chamber, differed on average by about 4% compared to the values of these coefficients obtained without considering air humidity fluctuations. In the case of each analyzed sample, the linear descriptions of the variability of the diffusion coefficient had a less steep course when considering air humidity fluctuations in the climatic chamber during the calculation process.

Keywords: error minimization, moisture diffusion, sorption kinetics, wood

[1]MSc., Eng., Opole University of Technology, Faculty of Civil Engineering and Architecture, ul. Katowicka 48, 45-061 Opole, Poland, e-mail: a.drzymala@doktorant.po.edu.pl, ORCID: 0000-0002-6616-9373
[2]DSc., PhD., Eng., Opole University of Technology, Faculty of Civil Engineering and Architecture, ul. Katowicka 48, 45-061 Opole, Poland, e-mail: j.swirska-perkowska@po.edu.pl, ORCID: 0000-0002-5571-2748
[3]DSc., PhD., Eng., Opole University of Technology, Faculty of Mechanical Engineering, ul. S. Mikołajczyka 5, 45-271 Opole, Poland, e-mail: s.pochwala@po.edu.pl, ORCID: 0000-0002-8128-5495

1. Introduction

Wooden structures have a very low global warming potential (GWP) compared to masonry and reinforced concrete structures [1], which has a significant impact on the growing interest in wood construction today. Wood has a complex, heterogeneous structure, which results in its mechanical, physical, and chemical properties being orthotropic. The properties of wood also depend to a large extent on the moisture content, which is influenced by factors such as the value of the moisture diffusion coefficient and the relative humidity of the surrounding air. It is widely believed that in addition to natural resistance, the moisture content in wood is one of the most important factors determining the durability of wood in civil engineering applications [2]. A similar dependence is also observed for other building materials, such as sandstone, where subsequent wetting and drying cycles noticeably modify its fatigue life [3].

In construction practice, knowledge of the moisture sorption properties of wood is important for properly designed building structures. In hygroscopic conditions, wood tends to reach an equilibrium state with the moisture content in the environment, i.e., to achieve equilibrium moisture content [4].

Methods for measuring the moisture diffusion coefficient can be generally divided into stationary and non-stationary methods. In stationary methods, the parameters of the process do not change. The most popular stationary method is the cup method [5–8]. The measurement setup consists of a glass vessel that is closed with a sample. Inside the container, there is a saturated salt solution, which is used to maintain a constant humidity of the air under the sample. As a result of the difference in humidity above and below the sample, moisture flow occurs, which causes changes in the mass of the measuring set. When these changes stabilize over time, it can be assumed that a stationary state has been reached inside the sample. In [5], a modified cup method was proposed, allowing for a more precise analysis of moisture transport and sorption processes in wood. In this method, the use of a hygrostatic salt solution is abandoned. Instead, a small data logger is placed inside the vessel to monitor changes in relative humidity and temperature inside the dish during the test. At low moisture content in wood, stationary measurements can yield moisture diffusion coefficient values similar to those obtained from non-stationary measurements, but at higher moisture content, the results obtained from stationary methods are nearly twice as large as those from non-stationary measurements [9, 10].

In non-stationary methods, the flow of water vapour is induced by changing of humidity conditions in the sample environment. Two main types of non-stationary methods are distinguished: methods based on measuring the kinetics of moisture sorption and methods based on measuring moisture distribution. Examples of known methods based on the analysis of sorption kinetics include the Crank method and the Liu method. The basis for the analysis of sorption kinetics is measurements of the change in sample mass over time. The Crank method is based on solving the diffusion equation with a first kind boundary condition. Only measurement points from the initial range of the sorption kinetics curve, which align in a straight line, are considered in the calculations. The Liu method is based on solving the diffusion equation with a third kind boundary condition, which also allows for the consideration of phenomenon of moisture surface emission at sample boundaries [11] if the conditions under which the experiment is conducted permit it. The authors of the papers [12, 13] have found that calculations using the Liu method are less time-consuming but also less accurate than calculations using the Crank method.

Besides methods based on analytical solutions, there is a group of methods based on minimizing the error function between measured and calculated calculated increments of mass samples over time. The application of the error function minimization method requires assuming a functional dependence of the moisture diffusion coefficient on the moisture concentration in the material [14]. In the literature, this dependence is usually expressed as exponential functions with different types of moisture functions in the exponent, such as linear [15, 16], quadratic [15, 17, 18], cubic polynomials [17], or hyperbolic [16]. Whereas, authors of other studies assume that the moisture diffusion coefficient is constant within a certain range of material moisture content [15, 16, 18–21] or takes the form of a linear function of moisture content [16]. Some researchers analyze different forms of the above-mentioned functions and choose the one that yields the lowest value of the error function [15, 16].

Another type of non-stationary method is those based on moisture distribution measurements. The essence of these methods is to solve the coefficient inverse problem, which is why they are also called inverse methods. Moisture distribution measurements in a sample can be classified into destructive and non-destructive techniques. An example of a destructive method is the gravimetric method. Non-destructive methods include nuclear magnetic resonance (NMR) [22–24], magnetic resonance imaging (MRI) [22], computed tomography (CT) [22, 25], and neutron imaging (NI) [26].

In this study, a method based on minimizing the error function was used to determine the moisture diffusion coefficient, which relies on measuring the kinetics of moisture sorption. Since there was intensive air movement in the climatic chamber, the moisture diffusion coefficient for each sample was sought assuming first kind boundary conditions (external mass transfer resistances were negligibly small). Four types of variability of the diffusion coefficient with material moisture content were analyzed namely constant, linear, quadratic, and exponential functions. The error function described the difference between the calculated and measured mass increases of sample at different moments during the sorption process. As it is known, a significant problem during studies of kinetics of the sorption process and drying is the fluctuations of parameters in the climatic chamber, especially during weighing samples when the chamber needs to be turned off [27–29]. The authors of this study performed calculations for each sample twice: once assuming constant air humidity in the chamber, and the other taking into account fluctuations in humidity recorded using a sensor placed near the samples. This allowed for the estimation of the impact of air humidity fluctuations in the chamber on the values of the determined of moisture diffusion coefficients in wood.

Since timber obtained from coniferous species is commonly used as a building material in Poland, samples of pine ordinary were selected for the study. Measurements of samples mass increases over time were conducted at a step change in relative air humidity from 0% to 32%. This is the first of three stages of the study planned by the authors.

2. Materials and methods

2.1. Experimental studies

The samples were obtained from pine ordinary wood (Pinus sylvestris) harvested from the lowland region of Poland. Seven samples were prepared in tangential (T) and radial (R) directions with approximate dimensions of $30 \times 30 \times 20$ mm each. The samples were then transferred to a heating chamber and dried to a constant mass (the conditioning process lasted approximately three months). To induce mass flow in only one selected direction in the samples, the dried samples were sealed on four sides with aluminum vapour-tight foil. After sealing, the samples were put back to the drying chamber to eliminate any moisture absorbed from the surroundings during insulation.

The dried and insulated samples were then transferred from the drying chamber to a climatic chamber with a predetermined relative humidity of 30% (±2%) and temperature of 23°C (±1°C), initiating the moisture sorption process in the samples. A temperature and humidity probe connected to a data logger was placed near the samples right after removal them from the drying chamber, recording the ambient air parameters at a frequency of every 5 minutes. Changes in sample mass over time were measured using a balance (with an accuracy of ±0.002 grams) placed inside the chamber. The measurement set-up is presented in Fig. 1. The measurement frequency ranged from every 2 hours to once every 10 days, gradually extending the time between weighings as the rate of mass gain in the samples decreased. During the measurements, the climatic chamber had to be turned off, and one weighing cycle lasted from 20 to 30 minutes. The entire experiment took approximately 7 months to complete. A graph showing air humidity fluctuations in the chamber during the study period is presented in Fig. 2.

Fig. 1. Samples and measurement setup inside the climatic chamber

As a result of the experiment, sorption curves of individual samples were obtained, which are presented in Fig. 3 and Fig. 4.

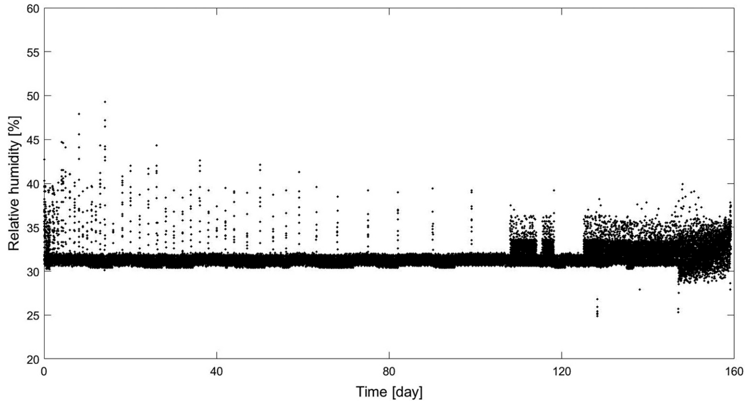

Fig. 2. Fluctuations of air humidity in the chamber during the experiment

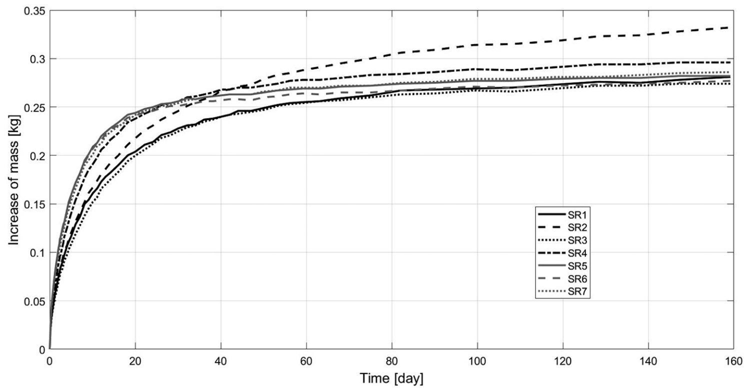

Fig. 3. Sorption kinetics curves for pine samples in the radial direction

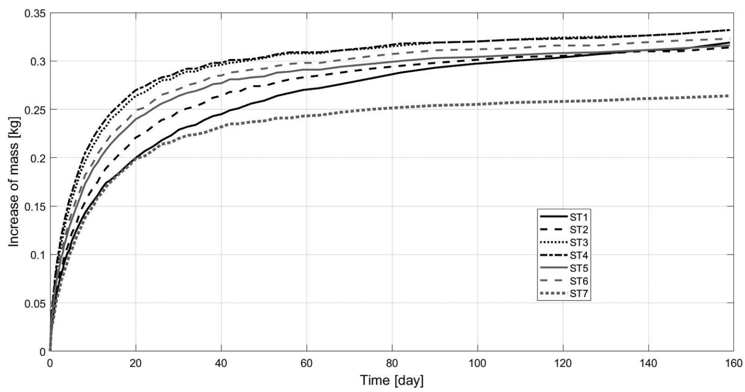

Fig. 4. Sorption kinetics curves for pine samples in the tangential direction

2.2. Mathematical model

In the analyzed case, the moisture flow through the samples occurred in the tangential (T) or radial (R) direction and was one-dimensional. The equation describing the mass diffusion process within the samples is given by the relation

$$\frac{\partial C^w}{\partial t} = \frac{\partial D_I^w}{\partial x}\frac{\partial C^w}{\partial x} + D_I^w \frac{\partial^2 C^w}{\partial x^2}, \quad I = R, T \tag{2.1}$$

where: I – direction of moisture flow in wood (R or T), C^w – moisture concentration in the sample (water mass in the sample relative to the mass of the dry sample) [kg/kg], D_I^w – moisture diffusion coefficient in the sample in the direction I [m^2/s], x – space coordinate coinciding with the axis of the sample [m], t – time [s].

Discretizing equation (2.1) according to the explicit scheme of finite difference method yields the following relation

$$\begin{aligned}\frac{C^w_{i,j} - C^w_{i,j-1}}{\Delta t} = {} & \frac{\left(D_I^w\right)_{i+1,j-1} - \left(D_I^w\right)_{i-1,j-1}}{2\Delta x}\frac{C^w_{i+1,j-1} - C^w_{i-1,j-1}}{2\Delta x} + \\ & + \left(D_I^w\right)_{i,j-1}\frac{C^w_{i+1,j-1} - 2C^w_{i,j-1} + C^w_{i-1,j-1}}{(\Delta x)^2}\end{aligned} \tag{2.2}$$

where: Δ means the increment, and subscripts i and j correspond to the spatial node and time point in the discretized space (x, t). The time step Δt changed during the calculations and each time it was selected in such a way that, on the one hand, the convergence condition of the explicit finite difference method was met, and on the other, that the change in moisture concentration from step to step at any spatial point was not greater than $0,02 \cdot \left(C^w_\infty - C^w_0\right)$.

In the considered case, the moisture distribution in the samples at the beginning of the process was homogeneous, hence the initial condition is given by

$$C^w_{i,0} = C^w_0 \tag{2.3}$$

where: C^w_0 is the initial moisture concentration in the sample.

Since the air in the climatic chamber where the sorption process was conducted is intensively mixed (air velocity is 3 m/s) and the samples were placed on a table under the fan, the external mass transfer resistances on the sorbing surfaces of the samples can be assumed to be negligibly small, and first kind boundary conditions were assumed on these surfaces

$$C^w_{1,j} = C^w_{n,j} = C^w_\infty \tag{2.4}$$

where: n is the number of nodes in the sample, a C^w_∞ – equilibrium moisture content in the sample corresponding to the humidity in the climatic chamber.

In the study, two cases were analyzed regarding the concentration values C^w_∞: one case assumed that the concentration is constant and equal to the moisture content in the sample, corresponding to the average air humidity in the chamber near the samples (32%). The other case assumed that the concentration fluctuates with the humidity fluctuations in the chamber, and its instantaneous values were determined based on the linearized by segments of the sorption isotherms of the respective sample. The linearization was performed based on the known equilibrium moisture content values of the samples at 32% and 60% relative air humidity.

2.3. The computational procedure involved in the study

Four types of the variability of the diffusion coefficient with moisture content were analyzed: constant, linear, quadratic, and exponential functions

$$D_I^w\left(C^w\right) = D_{Io} \tag{2.5}$$

$$D_I^w\left(C^w\right) = a_{Il} + b_{Il}C^w \tag{2.6}$$

$$D_I^w\left(C^w\right) = a_{Is} + b_{Is}C^w + c_{Is}\left(C^w\right)^2 \tag{2.7}$$

$$D_I^w\left(C^w\right) = a_{Ie}\exp\left(b_{Ie}C^w\right) \tag{2.8}$$

The values of the coefficients in the above functions were sought using the error function minimization method, utilizing the finite difference method. Software for calculating the moisture diffusion coefficient was written in MATLAB environment. Initially, an approximate value of the constant moisture diffusion coefficient was found using the method of numerical search throughout the domain and utilizing the analytical solution of equation (2.1). The search range was selected based on the diffusion coefficient values determined for individual wood samples using the $\sqrt{t}$-type Crank method (initial sorption). Next, the exact value of the constant moisture diffusion coefficient D_{Io} was determined, by minimizing the error function, using a numerical solution of the diffusion equation, and employing the Levenberg-Marquardt optimization algorithm. Subsequently, the coefficients in the linear (2.6) and exponential (2.8) functions were determined, with the starting point in the optimization procedure was in these cases a point $[D_{Io}, 0]$ (coefficient obtained in the previous step). On the other hand, the coefficients in the quadratic function (2.7) were determined by starting from the previously obtained linear function, i.e. from the starting point $[a_{Il}, b_{Il}, 0]$. During the calculations, error function was minimized which is the sum of absolute square deviations between the measured and calculated values

$$F = \sum_k \left(\Delta m_{e,k} - \Delta m_{o,k}\right)^2 \tag{2.9}$$

where $\Delta m_{e,k}$ denotes the measured mass increment of the sample at a given time k, and $\Delta m_{o,k}$ – calculated (for a given set of coefficients of the function $D_I^w\left(C^w\right)$), mass increment of the sample at the corresponding moment.

3. Results and discussion

The obtained sets of coefficients are presented in Tables 1 and 2, corresponding to the radial and tangential directions, respectively. For each model, two sets of coefficients are provided in the rows related to individual samples: the upper set (black colour) corresponds to calculations assuming constant humidity in the chamber during the experiment, while the lower set (grey colour) refers to results obtained taking into account humidity fluctuations in the surroundings of the samples. This way of presenting the results facilitates their comparison. Unfortunately, in the case of three samples in which the diffusion process was carried out in the radial direction

(SR5, SR6, and SR7), it was not possible to determine unambiguous values of the coefficients in quadratic functions $D_I^w(C^w)$ taking into account the variability of humidity conditions in the surroundings of the samples. In these cases, question marks were entered in the respective rows.

Tables 1 and 2 also include the values of the mean relative error of fitting the calculated curve to the experimental curve for a given set of coefficients, calculated according to the formula

$$e = \sum \frac{\left|\Delta m_{e,k} - \Delta m_{o,k}\right|}{\Delta m_{e,k}} \cdot \frac{100}{n_e} \tag{3.1}$$

where n_e is the number of time points at which measurements were taken.

Table 1. Values of coefficients in searched functions – radial direction

Model	**Sample**	**Determined functional coefficients**			$\boldsymbol{F}$ **[kg²]**	$\boldsymbol{e}$ **[%]**
		D_{To}/a_T **[m²/s]**	b_T **[m²/s]/[–]**	c_T **[m²/s]**		
Constant	SR1	$2.421 \cdot 10^{-11}$	–	–	$2.977 \cdot 10^{-9}$	9.08
		$2.544 \cdot 10^{-11}$	–	–	$1.973 \cdot 10^{-9}$	7.41
	SR2	$1.809 \cdot 10^{-11}$	–	–	$3.418 \cdot 10^{-9}$	9.43
		$1.900 \cdot 10^{-11}$	–	–	$2.405 \cdot 10^{-9}$	7.92
	SR3	$2.221 \cdot 10^{-11}$	–	–	$1.670 \cdot 10^{-9}$	6.80
		$2.336 \cdot 10^{-11}$	–	–	$0.953 \cdot 10^{-9}$	5.11
	SR4	$3.156 \cdot 10^{-11}$	–	–	$4.046 \cdot 10^{-9}$	8.62
		$3.292 \cdot 10^{-11}$	–	–	$2.693 \cdot 10^{-9}$	7.87
	SR5	$4.579 \cdot 10^{-11}$	–	–	$5.182 \cdot 10^{-9}$	9.46
		$4.746 \cdot 10^{-11}$	–	–	$3.965 \cdot 10^{-9}$	8.27
	SR6	$4.800 \cdot 10^{-11}$	–	–	$4.763 \cdot 10^{-9}$	9.05
		$4.965 \cdot 10^{-11}$	–	–	$3.040 \cdot 10^{-9}$	8.07
	SR7	$4.015 \cdot 10^{-11}$	–	–	$5.489 \cdot 10^{-9}$	9.76
		$4.164 \cdot 10^{-11}$	–	–	$3.763 \cdot 10^{-9}$	8.70
Linear	SR1	$9.095 \cdot 10^{-11}$	$-2.416 \cdot 10^{-9}$	–	$4.847 \cdot 10^{-11}$	2.63
		$8.030 \cdot 10^{-11}$	$-2.034 \cdot 10^{-9}$	–	$1.032 \cdot 10^{-10}$	2.98
	SR2	$6.247 \cdot 10^{-11}$	$-1.870 \cdot 10^{-9}$	–	$8.382 \cdot 10^{-11}$	3.20
		$5.767 \cdot 10^{-11}$	$-1.663 \cdot 10^{-9}$	–	$1.107 \cdot 10^{-10}$	3.52
	SR3	$7.353 \cdot 10^{-11}$	$-1.506 \cdot 10^{-9}$	–	$9.428 \cdot 10^{-11}$	2.86
		$6.910 \cdot 10^{-11}$	$-1.362 \cdot 10^{-9}$	–	$9.081 \cdot 10^{-11}$	2.92
	SR4	$1.176 \cdot 10^{-10}$	$-3.225 \cdot 10^{-9}$	–	$2.885 \cdot 10^{-10}$	5.76
		$9.834 \cdot 10^{-11}$	$-2.529 \cdot 10^{-9}$	–	$4.333 \cdot 10^{-10}$	5.39
	SR5	$1.706 \cdot 10^{-10}$	$-3.969 \cdot 10^{-9}$	–	$4.472 \cdot 10^{-10}$	4.45
		$1.199 \cdot 10^{-10}$	$-2.951 \cdot 10^{-9}$	–	$9.359 \cdot 10^{-10}$	5.61

Continued on next page

Table 1 – *Continued from previous page*

Model	**Sample**	**Determined functional coefficients**			F **[kg^2]**	e **[%]**
		D_{To}/a_T **[m^2/s]**	b_T **[m^2/s]/[–]**	c_T **[m^2/s]**		
	SR6	$1.796 \cdot 10^{-10}$	$-3.983 \cdot 10^{-9}$	–	$5.164 \cdot 10^{-10}$	5.05
		$1.441 \cdot 10^{-10}$	$-3.143 \cdot 10^{-9}$	–	$8.334 \cdot 10^{-10}$	5.25
	SR7	$1.435 \cdot 10^{-10}$	$-3.787 \cdot 10^{-9}$	–	$4.498 \cdot 10^{-10}$	4.77
		$1.521 \cdot 10^{-10}$	$-3.163 \cdot 10^{-9}$	–	$8.242 \cdot 10^{-10}$	5.52
Square	SR1	$7.578 \cdot 10^{-11}$	$-1.164 \cdot 10^{-9}$	$-2.369 \cdot 10^{-10}$	$4.228 \cdot 10^{-11}$	2.45
		$8.030 \cdot 10^{-11}$	$-2.034 \cdot 10^{-9}$	$1.725 \cdot 10^{-11}$	$1.029 \cdot 10^{-10}$	2.98
	SR2	$7.964 \cdot 10^{-11}$	$-3.575 \cdot 10^{-9}$	$3.827 \cdot 10^{-8}$	$6.485 \cdot 10^{-11}$	3.31
		$5.781 \cdot 10^{-11}$	$-1.672 \cdot 10^{-9}$	$-1.063 \cdot 10^{-10}$	$1.093 \cdot 10^{-10}$	3.51
	SR3	$1.975 \cdot 10^{-11}$	$-2.148 \cdot 10^{-9}$	$-5.643 \cdot 10^{-8}$	$2.359 \cdot 10^{-11}$	1.77
		$5.782 \cdot 10^{-11}$	$-5.388 \cdot 10^{-10}$	$-1.344 \cdot 10^{-8}$	$6.285 \cdot 10^{-11}$	2.61
	SR4	$7.593 \cdot 10^{-11}$	$-1.528 \cdot 10^{-9}$	$-5.39 \cdot 10^{-8}$	$2.734 \cdot 10^{-11}$	4.62
		$9.876 \cdot 10^{-11}$	$-2.531 \cdot 10^{-9}$	$-5.501 \cdot 10^{-10}$	$4.197 \cdot 10^{-10}$	5.37
	SR5	$1.715 \cdot 10^{-10}$	$-3.972 \cdot 10^{-9}$	$-6.379 \cdot 10^{-10}$	$4.212 \cdot 10^{-10}$	4.40
		?	?	?	?	?
	SR6	$1.806 \cdot 10^{-10}$	$-3.986 \cdot 10^{-9}$	$-6.333 \cdot 10^{-10}$	$4.923 \cdot 10^{-10}$	5.02
		?	?	?	?	?
	SR7	$1.442 \cdot 10^{-10}$	$-3.790 \cdot 10^{-9}$	$-6.899 \cdot 10^{-10}$	$4.249 \cdot 10^{-10}$	4.72
		?	?	?	?	?
Exponential	SR1	$2.151 \cdot 10^{-10}$	–88.681	–	$2.303 \cdot 10^{-10}$	4.14
		$1.794 \cdot 10^{-10}$	–79.555	–	$1.853 \cdot 10^{-10}$	4.01
	SR2	$1.305 \cdot 10^{-10}$	–93.238	–	$1.069 \cdot 10^{-10}$	3.88
		$1.147 \cdot 10^{-10}$	–85.385	–	$1.066 \cdot 10^{-10}$	4.02
	SR3	$1.369 \cdot 10^{-10}$	–58.457	–	$2.333 \cdot 10^{-10}$	3.56
		$1.057 \cdot 10^{-10}$	–48.595	–	$1.801 \cdot 10^{-10}$	3.43
	SR4	$2.502 \cdot 10^{-10}$	–88.253	–	$8.574 \cdot 10^{-10}$	7.31
		$2.047 \cdot 10^{-10}$	–77.845	–	$6.921 \cdot 10^{-10}$	6.92
	SR5	$6.376 \cdot 10^{-10}$	–94.001	–	$1.238 \cdot 10^{-9}$	7.20
		$4.885 \cdot 10^{-10}$	–82.801	–	$9.278 \cdot 10^{-10}$	6.55
	SR6	$6.299 \cdot 10^{-10}$	–87.374	–	$1.388 \cdot 10^{-9}$	7.83
		$4.687 \cdot 10^{-10}$	–75.684	–	$1.032 \cdot 10^{-9}$	7.14
	SR7	$4.464 \cdot 10^{-10}$	–100.115	–	$1.227 \cdot 10^{-9}$	7.63
		$3.642 \cdot 10^{-10}$	–89.865	–	$9.805 \cdot 10^{-10}$	7.14

Table 2. Values of coefficients in searched functions – tangential direction

Model	Sample	Determined functional coefficients			F [kg^2]	e [%]
		D_{To}/a_T [m^2/s]	b_T [m^2/s]/[–]	c_T [m^2/s]		
Constant	ST1	$1.562 \cdot 10^{-11}$	–	–	$3.573 \cdot 10^{-9}$	10.18
		$1.603 \cdot 10^{-11}$	–	–	$2.760 \cdot 10^{-9}$	9.82
	ST2	$2.059 \cdot 10^{-11}$	–	–	$2.827 \cdot 10^{-9}$	8.32
		$2.147 \cdot 10^{-11}$	–	–	$1.958 \cdot 10^{-9}$	7.60
	ST3	$3.169 \cdot 10^{-11}$	–	–	$9.179 \cdot 10^{-9}$	8.83
		$3.308 \cdot 10^{-11}$	–	–	$3.306 \cdot 10^{-9}$	7.96
	ST4	$3.426 \cdot 10^{-11}$	–	–	$5.572 \cdot 10^{-9}$	9.30
		$3.562 \cdot 10^{-11}$	–	–	$3.802 \cdot 10^{-9}$	8.49
	ST5	$2.449 \cdot 10^{-11}$	–	–	$3.826 \cdot 10^{-9}$	8.27
		$2.559 \cdot 10^{-11}$	–	–	$2.632 \cdot 10^{-9}$	8.57
	ST6	$2.700 \cdot 10^{-11}$	–	–	$4.336 \cdot 10^{-9}$	8.35
		$2.820 \cdot 10^{-11}$	–	–	$2.992 \cdot 10^{-9}$	7.52
	ST7	$2.403 \cdot 10^{-11}$	–	–	$1.930 \cdot 10^{-9}$	7.00
		$2.515 \cdot 10^{-11}$	–	–	$1.309 \cdot 10^{-9}$	7.49
Linear	ST1	$5.665 \cdot 10^{-11}$	$-1.860 \cdot 10^{-9}$	–	$2.182 \cdot 10^{-10}$	5.81
		$4.124 \cdot 10^{-11}$	$-1.177 \cdot 10^{-9}$	–	$6.861 \cdot 10^{-10}$	7.05
	ST2	$7.220 \cdot 10^{-11}$	$-1.927 \cdot 10^{-9}$	–	$8.699 \cdot 10^{-11}$	4.31
		$5.500 \cdot 10^{-11}$	$-1.294 \cdot 10^{-9}$	–	$3.467 \cdot 10^{-10}$	4.94
	ST3	$1.241 \cdot 10^{-10}$	$-3.326 \cdot 10^{-9}$	–	$2.724 \cdot 10^{-10}$	5.20
		$8.657 \cdot 10^{-11}$	$-2.015 \cdot 10^{-9}$	–	$9.266 \cdot 10^{-10}$	5.51
	ST4	$1.332 \cdot 10^{-10}$	$-3.657 \cdot 10^{-9}$	–	$2.747 \cdot 10^{-10}$	5.04
		$9.100 \cdot 10^{-11}$	$-2.151 \cdot 10^{-9}$	–	$1.206 \cdot 10^{-9}$	6.06
	ST5	$9.110 \cdot 10^{-11}$	$-2.528 \cdot 10^{-9}$	–	$2.183 \cdot 10^{-10}$	6.01
		$6.647 \cdot 10^{-11}$	$-1.615 \cdot 10^{-9}$	–	$6.360 \cdot 10^{-10}$	6.07
	ST6	$1.021 \cdot 10^{-10}$	$-2.835 \cdot 10^{-9}$	–	$1.876 \cdot 10^{-10}$	4.50
		$7.266 \cdot 10^{-11}$	$-1.753 \cdot 10^{-9}$	–	$7.476 \cdot 10^{-10}$	4.92
	ST7	$8.145 \cdot 10^{-11}$	$-1.800 \cdot 10^{-9}$	–	$3.710 \cdot 10^{-10}$	7.30
		$6.827 \cdot 10^{-11}$	$-1.383 \cdot 10^{-9}$	–	$4.084 \cdot 10^{-10}$	7.06
Square	ST1	$9.319 \cdot 10^{-11}$	$-5.758 \cdot 10^{-9}$	$9.442 \cdot 10^{-8}$	$1.335 \cdot 10^{-10}$	5.93
		$4.124 \cdot 10^{-11}$	$-1.177 \cdot 10^{-9}$	$-1.371 \cdot 10^{-11}$	$6.854 \cdot 10^{-10}$	7.05
	ST2	$5.006 \cdot 10^{-11}$	$-1.702 \cdot 10^{-11}$	$-3.764 \cdot 10^{-8}$	$6.700 \cdot 10^{-11}$	3.81
		$5.500 \cdot 10^{-11}$	$-1.294 \cdot 10^{-9}$	$-1.242 \cdot 10^{-11}$	$3.462 \cdot 10^{-10}$	4.94
	ST3	$1.114 \cdot 10^{-10}$	$-2.276 \cdot 10^{-9}$	$-1.988 \cdot 10^{-8}$	$2.254 \cdot 10^{-10}$	4.94
		$8.657 \cdot 10^{-11}$	$-2.015 \cdot 10^{-9}$	$-1.847 \cdot 10^{-11}$	$9.258 \cdot 10^{-10}$	5.51

Continued on next page

Table 2 – *Continued from previous page*

Model	Sample	Determined functional coefficients			F [kg^2]	e [%]
		D_{To}/a_T [m^2/s]	b_T [m^2/s]/[–]	c_T [m^2/s]		
Square	ST4	$1.340 \cdot 10^{-10}$	$-3.652 \cdot 10^{-9}$	$-9.796 \cdot 10^{-10}$	$2.687 \cdot 10^{-10}$	5.10
		$9.101 \cdot 10^{-11}$	$-2.151 \cdot 10^{-9}$	$-2.055 \cdot 10^{-11}$	$1.205 \cdot 10^{-9}$	6.06
	ST5	$6.928 \cdot 10^{-11}$	$-6.263 \cdot 10^{-10}$	$-3.786 \cdot 10^{-8}$	$1.437 \cdot 10^{-10}$	5.31
		$6.647 \cdot 10^{-11}$	$-1.615 \cdot 10^{-9}$	$-1.570 \cdot 10^{-11}$	$6.354 \cdot 10^{-10}$	6.07
	ST6	$8.551 \cdot 10^{-11}$	$-1.394 \cdot 10^{-9}$	$-2.854 \cdot 10^{-8}$	$1.346 \cdot 10^{-10}$	4.02
		$7.266 \cdot 10^{-11}$	$-1.753 \cdot 10^{-9}$	$-1.698 \cdot 10^{-11}$	$7.469 \cdot 10^{-10}$	4.92
	ST7	$2.616 \cdot 10^{-11}$	$-2.203 \cdot 10^{-9}$	$-6.625 \cdot 10^{-8}$	$1.893 \cdot 10^{-10}$	5.80
		$6.828 \cdot 10^{-11}$	$-1.383 \cdot 10^{-9}$	$-1.147 \cdot 10^{-11}$	$4.082 \cdot 10^{-10}$	7.06
Exponential	ST1	$1.329 \cdot 10^{-10}$	–108.933	–	$1.392 \cdot 10^{-10}$	6.02
		$1.218 \cdot 10^{-10}$	–103.077	–	1.30710^{-10}	6.41
	ST2	$1.495 \cdot 10^{-10}$	–82.036	–	$2.565 \cdot 10^{-10}$	5.55
		$1.284 \cdot 10^{-10}$	–74.293	–	$2.388 \cdot 10^{-10}$	5.77
	ST3	$3.023 \cdot 10^{-10}$	–91.549	–	$9.148 \cdot 10^{-10}$	6.83
		$2.474 \cdot 10^{-10}$	–81.739	–	$7.319 \cdot 10^{-10}$	6.61
	ST4	$3.448 \cdot 10^{-10}$	–96.937	–	$1.052 \cdot 10^{-9}$	7.09
		$2.845 \cdot 10^{-10}$	–87.191	–	$8.404 \cdot 10^{-10}$	6.81
	ST5	$1.979 \cdot 10^{-10}$	–88.883	–	$6.407 \cdot 10^{-10}$	7.42
		$1.664 \cdot 10^{-10}$	–79.837	–	$5.403 \cdot 10^{-10}$	7.39
	ST6	$2.307 \cdot 10^{-10}$	–91.197	–	$6.644 \cdot 10^{-10}$	6.04
		$1.950 \cdot 10^{-10}$	–82.409	–	$5.510 \cdot 10^{-10}$	5.92
	SR7	$1.444 \cdot 10^{-10}$	–61.501	–	$6.044 \cdot 10^{-10}$	7.88
		$1.152 \cdot 10^{-10}$	–52.271	–	$5.320 \cdot 10^{-10}$	7.98

As in each of the analyzed cases of humidity conditions, the linear and quadratic models showed the best fit to the experimental curves, a comparison of linear and quadratic functions obtained for individual samples is presented in Fig. 5–12, respectively for the assumption of constant and variable air humidity in the climatic chamber.

Additionally, for two selected samples, in which the diffusion of water vapour in the radial (SR4) and tangential (ST5) directions were considered, the course of all determined functions describing the relation $D_I^w(C^w)$ for the mentioned samples were illustrated in Fig. 13 and 14. The principle of selecting samples was based on the criterion that the determined constant diffusion coefficient for them was located in the middle of the range of variability of this coefficient within the set of all analyzed samples. For the same samples, the fitting of experimental curves to calculated curves was presented in Fig. 15, 16 (SR4) and 17, 18 (ST5), first assuming constant conditions in the chamber and then taking into account their variability.

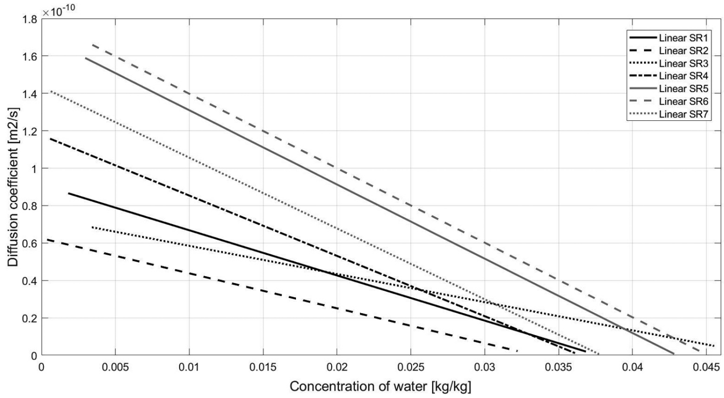

Fig. 5. Comparison of linear functions $D_I^w\,(C^w)$ – pine, radial direction, constant humidity

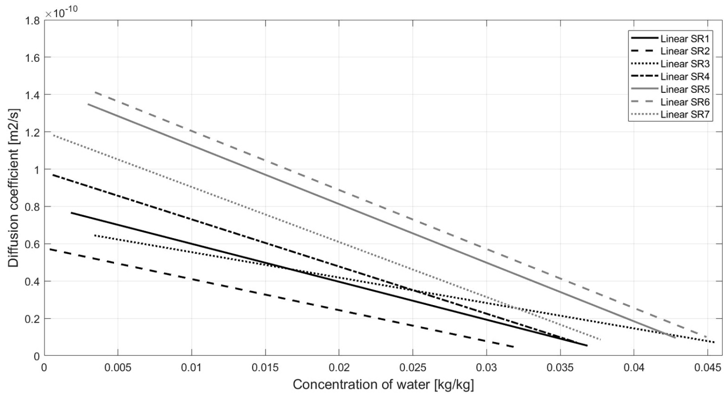

Fig. 6. Comparison of linear functions $D_I^w\,(C^w)$ – pine, radial direction, variable humidity

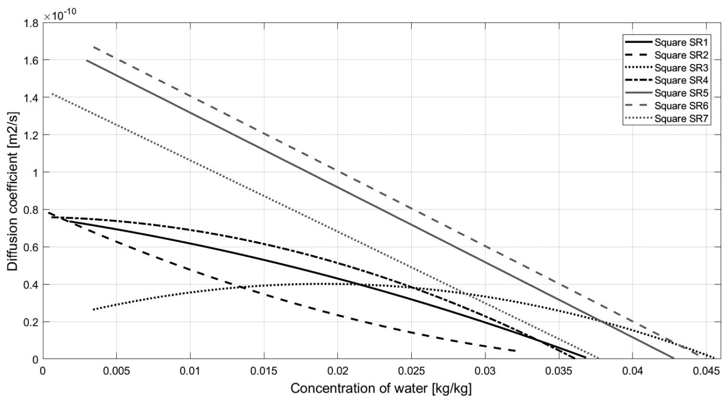

Fig. 7. Comparison of quadratic functions $D_I^w\,(C^w)$ – pine, radial direction, constant humidity

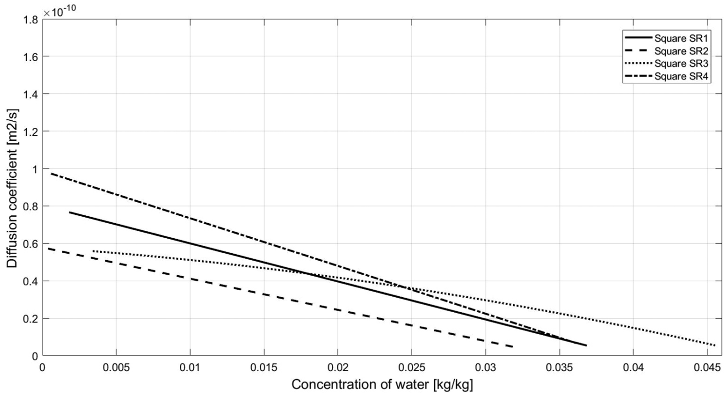

Fig. 8. Comparison of quadratic functions $D_I^w(C^w)$ – pine, radial direction, variable humidity

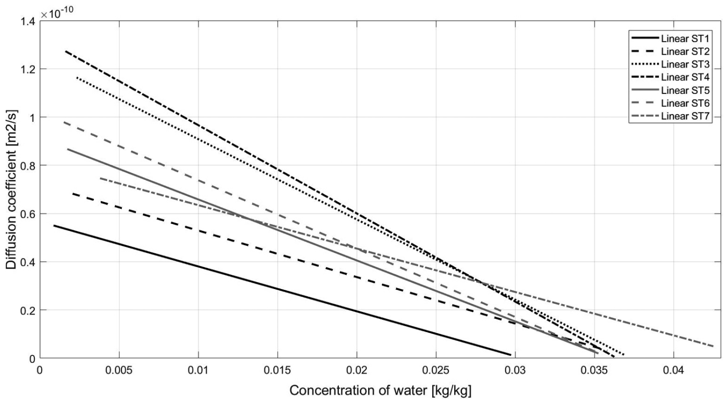

Fig. 9. Comparison of linear functions $D_I^w(C^w)$ – pine, tangential direction, constant humidity

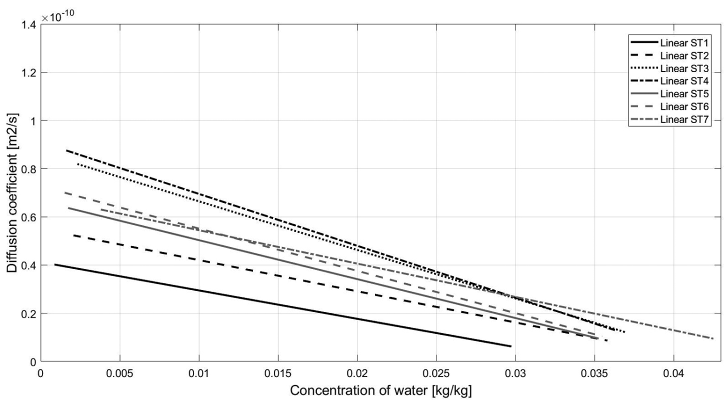

Fig. 10. Comparison of linear functions $D_I^w(C^w)$ – pine, tangential direction, variable humidity

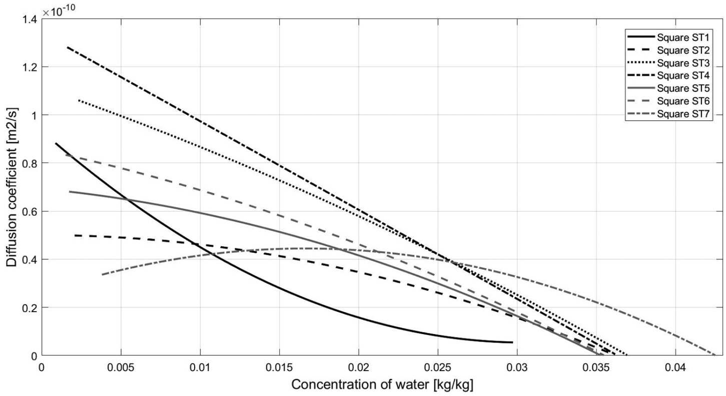

Fig. 11. Comparison of quadratic functions $D_I^w(C^w)$ – pine, tangential direction, constant humidity

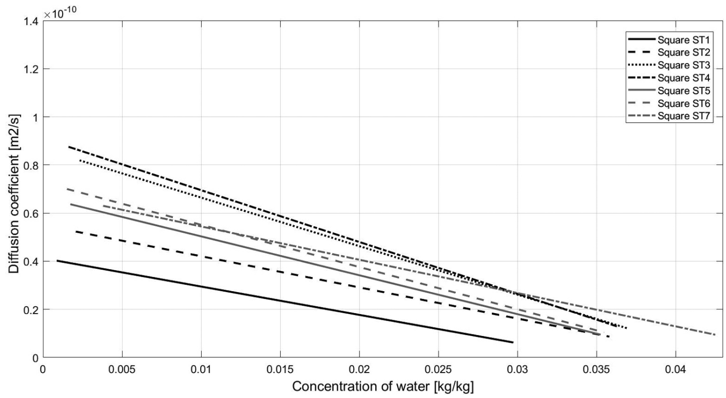

Fig. 12. Comparison of quadratic functions $D_I^w(C^w)$ – pine, tangential direction, variable humidity

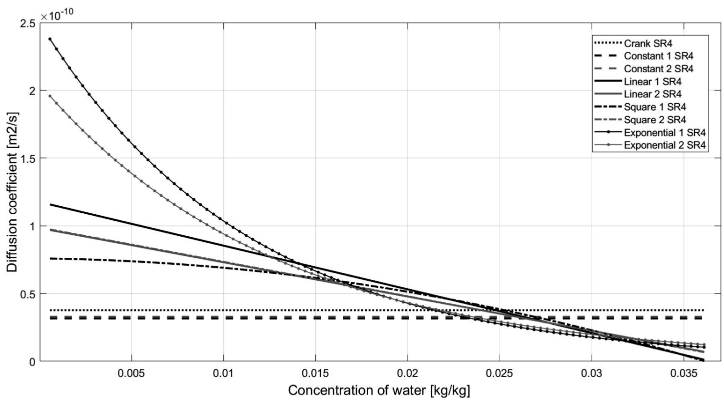

Fig. 13. Comparison of the course of individual functions $D_I^w(C^w)$ in the case of SR4 sample

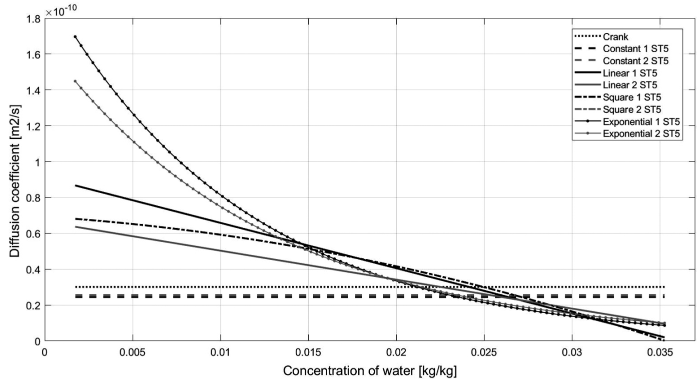

Fig. 14. Comparison of the course of individual functions $D_I^w\,(C^w)$ in the case of ST5 sample

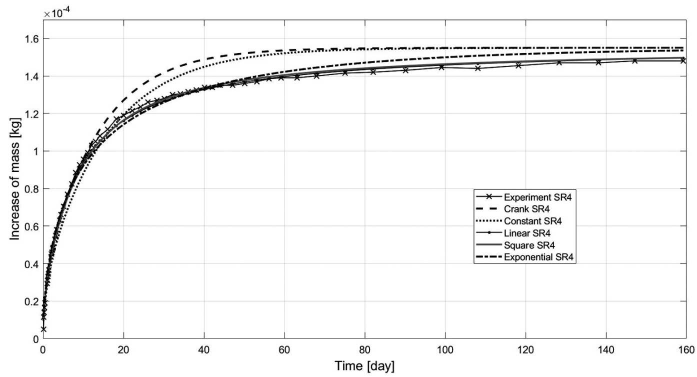

Fig. 15. Fitting of calculated curves corresponding to individual models to the experimental curve – SR4 sample, constant humidity

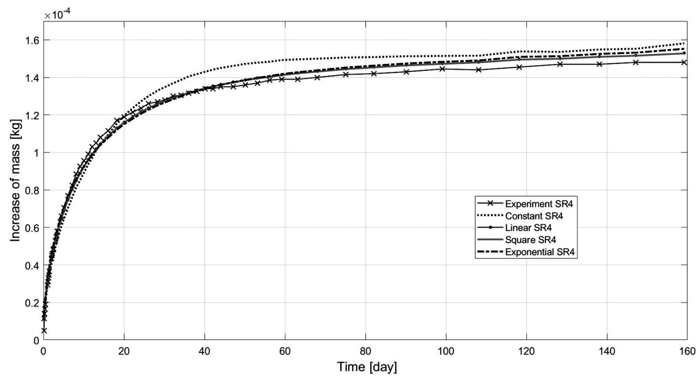

Fig. 16. Fitting of calculated curves corresponding to individual models to the experimental curve – SR4 sample, variable humidity

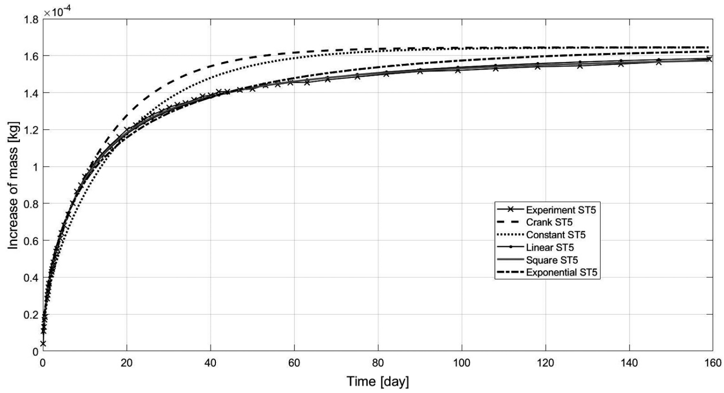

Fig. 17. Fitting of calculated curves corresponding to individual models to the experimental curve – ST5 sample, constant humidity

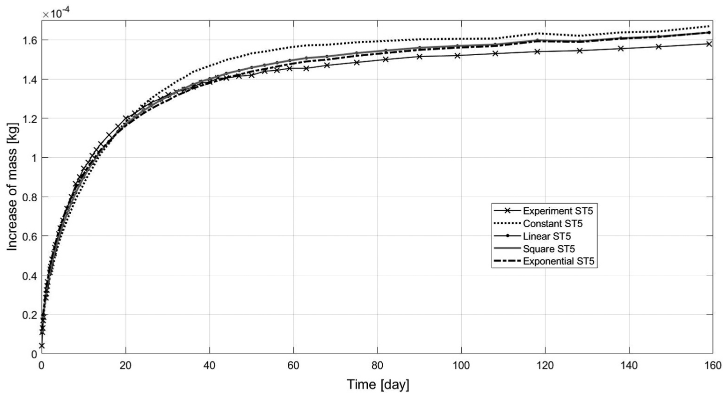

Fig. 18. Fitting of calculated curves corresponding to individual models to the experimental curve – ST5 sample, variable humidity

Comparing the values of the error functions presented in Table 1, it can be observed that in all considered cases, a decrease in the value of the error function F by over one order of magnitude was achieved when changing the dependence of $D_I^w\,(C^w)$ from constant to linear. The transition from linear to quadratic model is accompanied by a further decrease in the value of the error function, but the improvement of fitting of calculated curves to experimental curves is slight in this case. The exponential variability model of $D_I^w\,(C^w)$ [15, 16] often proposed in the literature results in a reduction of the error function value compared to the constant diffusion coefficient model, but the fitting of calculated curves to experimental curves is worse than in the case of the linear model.

As shown in Figures 5, 6, 9, and 10, for both analyzed diffusion directions and both considered humidity conditions in the chamber, the obtained diffusion coefficient is a decreasing function of material humidity. This result contradicts the common belief that in the case of transverse diffusion, this process is mainly realized through the diffusion of bound water in cell walls, and its intensity increases with the increase of material humidity [30]. Other researchers have also obtained decreasing diffusion coefficients with increasing material humidity in transverse directions: for pine ordinary in the radial direction – Olek and Weres [15], for common beech in the tangential direction – Olek, Perré, and Weres [18], for common beech in transverse directions – Sánchez-Ferrer, Engelhardt i Richter [31]. The tendency for the moisture diffusion coefficient to decrease with the moisture content of the material in the transverse directions can also be observed (at ambient temperature of 25°C) for the wood of radiata pine, tasmanian oak, slash pine, pacific teak and eucalyptus pilularis in work [32].

According to the data presented in Table 1, it can be observed that taking into account humidity fluctuations in the climatic chamber resulted in an increase in the constant diffusion coefficient values for each of the tested samples. This increase averaged 4.33% in the radial direction and 4.40% in the tangential direction. The change in the value of the coefficient D_I^w was accompanied by an average decrease in the error function F by 34.67% and 34,81% respectively, compared to the values of this function obtained assuming a constant value of C_∞^w during the process. Similarly, for the exponential model, an improvement in the fit of computational curves to experimental curves was observed for all tested samples after taking into account the fluctuations of equilibrium humidity C_∞^w with air humidity in the chamber. However, the reduction in the error function was smaller in this case, averaging 18.97% – in the radial direction and 13,98% – in the tangential direction. A decrease in the exponent coefficient was also observed for all analyzed samples, which results in a less steep course of $D_I^w\,(C^w)$ curves.

In the case of linear and quadratic models, a slight reduction in the improvement of fitting computational curves to experimental curves is usually observed after taking into account humidity fluctuations in the chamber. This is because in this case, during the optimization process, a wider range of humidity in which the sample can be found is taken into account, hence additional constraints on the set of coefficients in the function $D_I^w\,(C^w)$, are imposed to prevent the diffusion coefficient D_I^w from taking negative values throughout the entire range of humidity. For these reasons, the linear functions obtained as a result of optimization taking into account humidity fluctuations in the chamber have a less steep course compared to the functions obtained for individual samples assuming constant humidity.

4. Conclusions

In the study, the influence of taking into account humidity fluctuations in a climatic chamber during the sorption process on the computed values of functional coefficients appearing in various variability models, was analyzed $D_I^w\,(C^w)$. The relation between the moisture diffusion coefficient and material humidity was modelled as a constant, linear, quadratic, and exponential function. Tests of sorption kinetics were conducted on samples of pine ordinary in the radial and tangential directions, with an average air humidity in the chamber set at 32%.

The conducted analyses lead to the following conclusions:

1. Within the analyzed range of humidity, the moisture diffusion coefficient is a decreasing function of material humidity;

2. In the case of diffusion in transverse directions, the best fit of computational curves to experimental curves is achieved with a quadratic model of the variability of the moisture diffusion coefficient D_I^w with material humidity;
3. Taking into account humidity fluctuations in the climatic chamber improved the fit of computational curves to experimental curves in the case of constant and exponential dependency of the moisture diffusion coefficient $D_I^w(C^w)$;
4. The diffusion coefficients in the form of a constant calculated assuming variable humidity conditions in the chamber, differed on average by about 4% compared to the values of these coefficients obtained by neglecting air humidity fluctuations;
5. The determined lines describing the variability of $D_I^w(C^w)$ for each of the analyzed samples had a less steep slope when air humidity fluctuations in the climatic chamber were taken into account in the calculation process.

References

[1] Wrzesiński, K. Pawluk, M. Lendo-Siwicka, and J. Kowalski, "Analysis of technology, time and costs of three methods of building a single-family house: traditional brick, reinforced concrete prefabrication, timber frame", *Archives of Civil Engineering,* vol. 69, no. 2, pp. 23–39, 2023, doi: 10.24425/ace.2023.145250.

[2] D. Kržišnik, B. Lesar, N. Thaler, J. Planinšič, and M. Humar, "A study on the moisture performance of wood determined in laboratory and field trials", *European Journal of Wood and Wood Products*, vol. 78, pp. 219–235, 2020, doi: 10.1007/s00107-020-01506-z.

[3] Z. Jin-Song, L. Yu, Z. Heng-Liang, Y. Yu-Di, and B. Yi-Shun, "Experimental study on fatigue mechanical properties of sandstone after dry and wet cycle", *Archives of Civil Engineering*, vol. 68, no. 4, pp. 377–387, 2022, doi: 10.24425/ace.2022.143044.

[4] H. Neuhaus, *Budownictwo drewniane, Podręcznik inżyniera*. Rzeszów, Polska: PWT, 2008.

[5] J. Eitelberger and S. Svensson, "The sorption behaviour of wood studies by means of an improved cup method", *Transport in Porous Media*, vol. 92, pp. 321–335, 2012, doi: 10.1007/s11242-011-9905-8.

[6] B. Time, "Hygroscopic Moisture Transport in Wood", PhD thesis, Norwegian University of Science and Technology, Norway, 1998.

[7] L. Wadsö, "Studies of water vapor transport and sorption in wood", PhD thesis, Lund University, Sweden, 1993.

[8] Y. Liu, Z. Cao, Y. Wang, D. Wang, and J. Liu, "Experimental study of hygro-thermal characteristics of novel cement-cork mortars", *Construction and Building Materials*, vol. 271, art. no. 121901, 2021, doi: 10.1016/j.conbuildmat.2020.121901.

[9] P. Pérre, Ed. *Fundamentals of wood drying*. Nancy, France: A.R.BO.LOR., 2007.

[10] W. Sonderreger, M. Vecellio, P. Zwicker, and P. Niemz, "Combined bound water and water vapour diffusion of Norway spruce and European beech in and between the principal anatomical directions", *Holzforschung*, vol. 65, no. 6, pp. 819–828, 2011, doi: 10.1515/HF.2011.091.

[11] J. Świrska-Perkowska, *Adsorpcja i ruch wilgoci w porowatych materiałach budowlanych w warunkach izotermicznych*. Warszawa, Polska: Komitet Inżynierii Lądowej i Wodnej, Polska Akademia Nauk, 2012.

[12] H. Garbalińska, "Metoda czasu połówkowego w desorpcyjnych pomiarach współczynnika dyfuzji", in *IX Konferencja Naukowo-Techniczna Fizyka Budowli w Teorii i Praktyce, 23-26 czerwca 2003, Łódź-Słok, Polska*. Łódź: Politechniki Łódzka, 2003, pp. 157–163.

[13] N. Ramos, J. Delgado, and V. de Freitas, "Concentration dependent diffusion in building materials – application of different methods", *Defect and Diffusion Forum*, vol. 273-276, pp. 150–155, 2008, doi: 10.4028/www.scientific.net/DDF.273-276.150.

[14] Z. Perkowski, J. Świrska-Perkowska, and M. Gajda, "Comparison of moisture diffusion coefficients for pine, oak and linden wood", *Journal of Building Physics*, vol. 41, no. 2, pp. 135–161, 2017, doi: 10.1177/1744259116673967.

[15] W. Olek and J. Weres, "Effects of method of identification of the diffusion coefficient on accuracy of modelling bound water transfer in wood", *Transport in Porous Media*, vol. 66, pp. 135–144, 2007, doi: 10.1007/s11242-006-9010-6.

[16] W. Silva, L. Silva, V. Oliveira Farias, C. Silva e Silva, and J. Ataíde, "Three-dimensional numerical analysis of water transfer in wood: determination of an expression for the effective mass diffusivity", *Wood Science and Technology*, vol. 47, pp. 897–912, 2013, doi: 10.1007/s00226-013-0544-9.

[17] W. Kang, Y.H. Lee, W.Y. Chung, and H.L. Xu, "Parameter estimation of moisture diffusivity in wood by an inverse method", *Journal of Wood Science*, vol. 55, pp. 83–90, 2009, doi: 10.1007/s10086-008-1006-0.

[18] W. Olek, P. Perré, and J. Weres, "Implementation of a relaxation equilibrium term in the covective boundary condition for a better representation of the transient bound water diffusion in wood", *Wood Science and Technology*, vol. 45, pp. 677–691, 2011, doi: 10.1007/s00226-010-0399-2.

[19] R. Sargent, S. Riley, and L. Schöttle, "Measurement of dynamic sorption behaviour of small specimens of pinus radiata. Influence of wood type and moisture content on diffusion rate", *Maderas. Ciencia y Tecnologia*, vol. 12, no. 2, pp. 93–103, 2010, doi: 10.4067/SO718-221X2010000200004.

[20] S.Q. Shi, "Diffusion model Based on Fick's second law for the moisture absorption process in wood fiber-based composites: is it suitable or not?", *Wood Science and Technology*, vol. 41, pp. 645–658, 2007, doi: 10.1007/s00226-006-0123-4.

[21] W. Silva, L. Silva, C. Silva e Silva, P. Nascimento, "Optimization and simulation of drying processes using diffusion models: application to wood drying using forced air at low temperature", *Wood Science and Technology*, vol. 45, pp. 787–800, 2011, doi: 10.1007/s00226-010-0391-x.

[22] D.M. Nguyen, G. Almeida, T.M.L. Nguyen, J. Zhang, P. Lu, J. Colin, and P. Perré, "A Critical Review of Current Imaging Techniques to Investigate Water Transfers in Wood and Biosourced Materials", *Transport in Porous Media*, vol. 137, pp. 21–61, 2021, doi: 10.1007/s11242-020-01538-2.

[23] G. Almeida, S. Gagné, and R.E. Hernández, "A NMR study of water distribution in hardwoods at several equilibrium moisture contents", *Wood Science and Technology*, vol. 41, pp. 293–307, 2007, doi: 10.1007/s00226-006-0116-3.

[24] S.V. Dvinskikh, M. Henriksson, A.L. Mendicino, S. Fortino, and T. Toratti, "NMR imaging study and multi-Fickian numerical simulation of moisture transfer in Norway spruce samples", *Engineering Structures*, vol. 33, no. 11, pp. 3079–3086, 2011, doi: 10.1016/j.engstruct.2011.04.011.

[25] P. Perré, "A review of modern computational and experimental tools relevant to the feld of drying", *Drying Technology,* vol. 29, no. 13, pp. 1529–1541, 2011, doi: 10.1080/07373937.2011.580872.

[26] D. Mannes, W. Sonderegger, S. Hering, E. Lehmann, and P. Niemz, "Non-destructive determination and quantification of diffusion processes in wood by means of neutron imaging", *Holzforschung*, vol. 63, no. 5, pp. 589–596, 2009, doi: 10.1515/HF.2009.100.

[27] H. Garbalińska, S. J. Kowalski, and M. Staszak, "Moisture diffusivity in mortars of different water–cement ratios and in narrow ranges of air humidity changes", *International Journal of Heat and Mass Transfer*, vol. 56, no. 1-2, pp. 212–222, 2013, doi: 10.1016/j.ijheatmasstransfer.2012.09.026.

[28] M. Kamran and K. Sarkar, "Study of the isothermal drying characteristics of normal concrete subjected to low air velocity convection", *Journal of Building Engineering*, vol. 61, art. no. 105251, 2022, doi: 10.1016/j.jobe.2022.105251.

[29] A. Kucharczyk and K. Pawlik, "Modelling and experimental study of moisture transport in wood, taking into account diffusion and the accompanying adsorption of water vapour by cell walls", *MDPI Materials*, vol. 14, no. 1, pp. 1–18, 2021, doi: 10.3390/ma14010017.

[30] W. Kang, W.Y. Chung, C. Eom, and H. Yeo, "Some considerations in heterogeneous nonisothermal transport models for wood: a numerical study", *Journal of Wood Science*, vol. 54, pp. 267–277, 2008, doi: 10.1007/s10086-007-0938-0.

[31] A. Sánchez-Ferrer, M. Engelhardt, and K. Richter, "Anisotropic wood–water interactions determined by gravimetric vapor sorption experiments", *Cellulose*, vol. 30, pp. 3869–3885, 2023, doi: 10.1007/s10570-023-05093-z.

[32] A.A. Chiniforush, H. Valipour, and A. Akbarnezhad, "Water vapor diffusivity of engineered wood: Effect of temperature and moisture content", *Construction and Building Materials*, vol. 224, pp. 1040–1055, 2019, doi: 10.1016/j.conbuildmat.2019.08.013.

Wpływ fluktuacji wilgotności w komorze na obliczeniowe wartości współczynnika dyfuzji wilgoci w drewnie

Słowa kluczowe: drewno, dyfuzja wilgoci, kinetyka sorpcji, minimalizacja funkcji błędu

Streszczenie:

W zastosowaniach inżynierii lądowej, obok naturalnej odporności, zawartość wilgoci w drewnie jest jednym z najważniejszych czynników decydujących o trwałości drewna. Na poziom wilgotności drewna znaczący wpływ ma wartość współczynnika dyfuzji wilgoci. W pracy przeanalizowano wpływ uwzględnienia wahań wilgotności w komorze klimatycznej podczas procesu sorpcji na obliczeniowe wartości współ czynników funkcyjnych, występujących w różnych modelach zmienności współczynnika dyfuzji wraz z wilgotnością materiału. Zależność współczynnika dyfuzji wilgoci od koncentracji wilgoci w drewnie przyjmowano w postaci funkcji: stałej, liniowej, kwadratowej i eksponencjalnej. Współczynniki w poszukiwanych funkcjach znajdowano metodą minimalizacji funkcji błędu, w oparciu o pomiary kinetyki sorpcji wilgoci w próbkach sosny zwyczajnej w kierunku radialnym i stycznym, przy średniej wilgotności powietrza w komorze równej 32%. W wyniku przeprowadzonych obliczeń stwierdzono, że uwzględnienie wahań wilgotności powietrza w komorze klimatycznej poprawiło dopasowanie krzywych obliczeniowych do krzywych eksperymentalnych w przypadku modelu stałego i eksponencjalnego. Wartości współczynnika dyfuzji w postaci stałej, obliczone przy założeniu zmiennych warunków wilgotnościowych panujących w komorze, różniły się średnio o około 4% w stosunku do wartości tych współczynników uzyskanych przy pominięciu fluktuacji wilgotności powietrza. W przypadku każdej z analizowanych próbek proste, opisujące zmienność współczynnika dyfuzji, miały mniej stromy przebieg, jeżeli w procesie obliczeń uwzględniano wahania wilgotności powietrza w komorze klimatycznej.

Received: 2023-08-21, Revised: 2023-10-24